Parametric Effects on Dryout of Propane in a Vertical Circular Mini-Channel

Muhammad H. MAQBOOL[1], Björn PALM[1*], Rahmatollah KHODABANDEH[1]

* Corresponding author: Tel.: +46 (0)8 790 7453; Fax: +46 (0)8 20 41 61; Email: bpalm@energy.kth.se
1: Applied Thermodynamics and Refrigeration, Royal Institute of Technology, KTH, Sweden.

Abstract This article presents dryout results of propane in a vertical circular mini channel made of stainless steel with an internal diameter of 1.70 mm and a heated length of 245 mm. The experiments are performed at three saturation temperatures of 23 ^{o}C, 33 ^{o}C and 43 ^{o}C. Mass flux is varied from 100 kg/m^{2}s to 500 kg/m^{2}s.The heat flux is increased in steps up to occurrence of dryout. The effect of different parameters such as mass flux, vapour quality and saturation temperature on the dryout heat flux is investigated. The results show that the dryout heat flux increases with the increase in mass flux and with the decrease of vapour quality. Almost no effect of saturation temperature on the dryout heat flux is observed. The generalised CHF correlations developed for macro and micro scale from the literature are compared with experimental results. Correlations developed by Callizo et al. (2008), Bowring (1972) and Katto and Ohno (1984) gave reasonably good predictions.

Keywords: Mini Channel, Dryout, Propane, CHF

1. Introduction

Flow boiling in mini and micro channels is presently one of the leading areas in boiling heat transfer research. Mini channels offer several advantages such as increased heat transfer, low fluid inventory and thereby increased safety when using flammable refrigerants, low cost and reduced size resulting in increased compactness etc. The main application areas of mini and micro channels include electronic cooling, AC systems in the automotive industry and biomedical engineering. Knowledge and technology can as well be transferred to heat pump and refrigeration systems. In the last two decades, the heat transfer research in mini channels has been focused on HFC refrigerants. The requirement to replace HFCs in near future due to environmental concerns has encouraged the research community to find potential natural refrigerants capable of replacing HFCs. Therefore in the last decade, several flow boiling studies have been done to capture the behaviour of natural refrigerants in mini channels.

CHF (critical heat flux) is referred to by some researchers, as the heat flux at which physical burnout of the test section occurs. Other researchers consider that CHF may not necessarily be accompanied with the physical burn out of the test section (Collier and Thome, 1994). The term dryout is used instead of CHF in this article as the power supply was shut down before physical burn out of the test section occurred. Dryout occurs when there is not enough liquid in the flow to wet the wall of the channel. The wall superheat temperature starts increasing and the heat transfer is deteriorated.

In designing a two phase mini-channel heat sink, it is necessary to know the dryout limitations for a secure operation of the heat exchanger.

Propane is one of the potential candidates to replace HFCs. Propane does not have any Ozone Depletion Potential (ODP) and has very low Global Warming Potential (GWP). It is non-toxic, chemically stable, and compatible with most materials used in HFC equipment and is miscible with commonly used compressor lubricants. Propane has very good thermodynamic and transport properties and also properties that closely resemble HFCs,

allowing it to be used without re-design of existing systems. However, the main concern with the use of propane is its high flammability which can be addressed by low fluid inventory, achieved by use of compact heat exchangers (Fernando et al. 2007).

Most of the investigations reported in the literature regarding CHF use water as working fluid. The main objectives of this study are to investigate dryout of propane in mini and micro channels and also to compare the predicting capabilities of well known correlations from the literature.

2. Literature Review

Lazarek and Black (1972) studied heat transfer, pressure drop and CHF using R113 as working fluid in a vertical circular mini channel of 3.15 mm internal diameter and heated lengths of 123 and 246 mm. Mass flux was varied from 232 to 740 kg/m^{2}s, heat flux from 93.1 to 336 kW/m^2, saturation temperature from 55.8 to 98.4 ^{o}C and inlet subcooling from 2.94 to 73.8 ^{o}C. The CHF was observed to occur at high vapor qualities (0.6-0.8). They also observed that the CHF was due to dryout of the liquid film at the exit of the test section. The new developed correlation predicted their experimental data with 5 % accuracy.

Tain et al. (1993) presented experimental CHF results for HCFCs and a HFCs. CHF tests were performed in a test section of 4.20 mm internal diameter and with varying heated length from 0.5 to 1 m. Mass flux was varied from 1000 to 4000 kg/m^{2}s. Most of the CHF data was observed in the annular flow regime. Finally they concluded that HFC-R134a, HCFC-123 and HCFC-22 were suitable replacements for CFCs regarding CHF.

Bowers and Mudawar (1994) presented CHF results of working fluid R113 in circular mini and micro channels. In this study, a mass flux ranging from 31 to 480 kg/m^{2}s, a saturation pressure of 138 kPa and an inlet subcooling from 10 K to 32 K were used. Contrary to previous studies found in the literature, no effect of inlet sub-cooling on CHF was observed.

Wojtan et al. (2006) presented experimental critical heat flux results in 0.5 and 0.8 mm internal diameter mini channel tubes with variable heating length from 20 to 70 mm. R134a and R245fa were used as working fluids. The tests were performed at two saturation temperatures, 30 and 35 ^{o}C, with mass flux ranging from 400 to 1600 kg/m^{2}s, heat flux from 3.2 to 1600 kW/m^2 and inlet sub cooling from 2 to 15 ^{o}C. The results showed increase in CHF with mass flux and no effect of sub cooling on CHF was observed. The comparison of experimental data with well known correlations showed that Katto and Ohno (1984) correlation predicted the data with MAD (Mean Absolute Deviation) of 32.8 %. A new correlation based on Katto and Ohno (1984) correlation was developed which predicted their experimental data with MAD of 7.6 %.

Kosar and Peles (2007) investigated CHF in a silicon based micro-channel heat sink for a heat flux ranging from 53 W/cm^2 to 196 W/cm^2, mass flux ranging from 291 kg/m^{2}s to 1118 kg/m^{2}s and for exit pressures ranging from 227 kPa to 520 kPa. Saturated flow boiling CHF was observed to increase with increase in mass flux and to decrease with increase in exit quality. CHF was reported to increase with increase in system pressure up to a certain value and then decreased. A new correlation was developed which captured the CHF trends with MAD of 3.8 %.

Ali (2010) performed experiments to determine dryout heat flux in vertical circular mini-channels with internal diameters of 1.22 mm and 1.70 mm and with a uniform heated length of 220 mm. R134a was used as working fluid. The test conditions were; mass flux ranging from 50 to 600 kg/m^{2}s, heat flux from 18 to 156 kW/m^2, saturation temperatures of 27 and 32 ^{o}C and inlet sub cooling of 3 ^{o}C. The dryout heat flux was observed to increase with mass flux and decrease with the decrease in tube diameter. The saturation temperature had minimal influence on the dryout heat flux. The experimental results were compared with CHF correlations where Bowring (1972) gave the best prediction with MAD of 13 %.

3. CHF Correlations

Kato and Ohno (1984) developed a CHF correlation which has been widely accepted and reported in literature. The functional form of the correlation for saturated CHF is;

$$\frac{q''_{CHF}}{Gi_{lv}} = f\left\{\frac{\rho_l}{\rho_v}, \frac{\sigma\rho_l}{G^2L}, \frac{L}{D_h}\right\} \quad (1)$$

In case of subcooling, the modified form of the correlation is;

$$\left(q''_{CHF}\right)_{sub} = q''_{CHF}\left\{1 + \frac{K\Delta i_{in}}{i_{lv}}\right\} \quad (2)$$

The value of K can be determined on the basis of different conditions and properties as described in detail by Kato and Ohno (1984)

Bowring (1972) suggested a correlation which can be written in mathematical form as;

$$q''_{CHF} = \frac{A' + 0.25DG\Delta i_{in}}{C' + L} \quad (3)$$

A′ and C′ are functions of properties and geometrical details which can be seen in detail in Bowring (1972).

Callizo et al. (2008) presented a correlation for micro channels by adjusting the coefficients in the Katto and Ohno (1984) correlation using least square regression analysis. The functional form of this correlation is;

$$\frac{q''_{CHF}}{Gi_{lv}} = 0.3216\left(\frac{\rho_v}{\rho_l}\right)^{0.084} We_l^{-0.034}\left(\frac{L}{D}\right)^{-0.942} \quad (4)$$

Wojtan et al. (2006) correlation was also based on Katto and Ohno (1984) correlation using new empirical factors on the basis of their experimental results of CHF in single circular uniformly heated microchannel.

$$\frac{q''_{CHF}}{Gi_{lv}} = 0.437\left(\frac{\rho_v}{\rho_l}\right)^{0.073} We_l^{-0.24}\left(\frac{L}{D}\right)^{-0.72} \quad (5)$$

Zhang et al. (2006) developed a CHF correlation on the basis of saturated flow boiling data of water at various operating conditions. The functional form of this correlation is;

$$\frac{q''_{CHF}}{Gi_{lv}} = 0.0352\left[We_D + 0.0119\left(\frac{\rho_v}{\rho_l}\right)^{0.361}\left(\frac{L}{D}\right)^{2.31}\right]^{-0.295}$$
$$\left(\frac{L}{D}\right)^{-0.311}\left[2.05\left(\frac{\rho_v}{\rho_l}\right)^{0.170} - x_{in}\right] \quad (6)$$

Bowers and Mudawar (1994) correlation can be written in mathematical form as;

$$\frac{q''_{CHF}}{Gi_{lv}} = 0.16\, We_l^{-0.19}\left(\frac{L}{D}\right)^{-0.54} \quad (7)$$

Qi et al. (2007) presented a CHF correlation on the basis of flow boiling in four mini and micro channels and can be formulated as;

$$\frac{q''_{CHF}}{Gi_{lv}} = (0.214 + 0.140Co)\left(\frac{\rho_v}{\rho_l}\right)^{0.133} We_l^{-0.333}\frac{1}{1+0.03^{L}/_{D}} \quad (8)$$

4. Experimental Set-up and Data Reduction

The experimental vertical mini channel test rig is shown in Figure 1. The experimental set-up consists of a closed loop: the subcooler, the magnetic gear pump, the Coriolis mass flow meter, the preheater, the test section and the condenser. The subcooler fully subcools the refrigerant to reduce the risk of cavitation in the magnetic gear pump. The subcooled refrigerant flows to the inlet of the magnetic gear pump (ISMATEC, type MCP-Z standard). The mass flow rate is controlled by adjusting the speed of the pump and is measured by a Coriolis mass flow meter (MicroMotion, DS006). The refrigerant then enters the preheater where it is heated up to the desired inlet temperature. The preheater consists of a heating coil wound around the stainless steel tube in which refrigerant flows. Before the entry of the test section, a filter of 7 micro meters is installed to restrict any particles to enter the test section. After passing through the test section, the refrigerant enters the condenser for condensation of the vapor to liquid. After the condenser the liquid enters the subcooler to complete the loop. The system pressure is maintained constant by a tank connected to main loop.

The system pressure is measured by an absolute pressure transducer (Druck PDCR 4060, 20 bar). A differential pressure

transducer (Druck PDCR 2160, 350mbar) is used to measure the pressure drop across the test section. The refrigerant temperatures at the inlet and the outlet of the test section are measured by T-type thermocouples. The test rig is insulated by thermal insulation to prevent heat loss to the surroundings. The outer wall temperatures of the test section are measured by T-type thermocouples. The thermocouples are attached to the outer wall of the test section after covering them with a special epoxy which is thermally conductive and electrically insulating. The inner wall temperatures are calculated from the measured outer wall temperatures by one dimensional heat conduction equation for cylindrical wall assuming steady state condition, uniform heat generation (Joule effect) in the tube wall and no heat loss to surroundings due to the well insulated wall (Owhaib, 2007). The test section consists of a stainless steel (AISI 316) tube with inner diameter of 1.70 mm and 245 mm in length. A glass tube of the same inner diameter as of test section is inserted after and before the test section to visualize the flow regime and to insulate the test section electrically and thermally from the test rig. The roughness of the test section was determined by scanning the inner surface using a method called conical stylus profilometry. Five profiles of the inner surface of test section were obtained. The scanned structure of the inner surface of the test section is shown in Figure 2. The details of the roughness test result are shown in table 1 where R_a represents the arithmetic mean roughness, R_v the maximum valley depth and R_p is the maximum peak height.

All tests are performed in steady state conditions. After achieving steady state conditions, the data is recorded by a data logger connected to a computer for almost five minutes and around 100 data points are recorded. The average values of these data points are used in the calculations.

All thermal and transport properties including enthalpy, density, viscosity and thermal conductivity of propane are calculated using REFPROP 7 developed by NIST (National Institute of Standards and Technology). The uncertainty propagation in the measurement of diameter, tube length, power input, temperature, pressure and mass flow rate is calculated by EES (Engineering Equation Solver) software. It uses the uncertainty propagation method suggested by Taylor and Kuyatt (1994). The uncertainties in the experimental results are tabulated in table 2.

The vapour quality at any vertical location (z) is determined from the heat transferred to the fluid as;

$$x_z = \frac{q''\cdot\pi D\cdot(Z-Z_{sat})}{A_c\cdot G\cdot i_{lv}} \quad (9)$$

Z is the desired location where vapour quality is estimated, Z_{sat} is the location where saturation conditions along the test section are reached and can be determined as;

$$z_{sat} = \frac{\dot{m}\cdot C_p\cdot(T_{sat}-T_{in})}{q''\cdot\pi D} \quad (10)$$

The Mean Absolute Deviation (MAD) is used to compare the experimental data with generalised correlations according to the following expression;

$$MAD = \frac{1}{N}\sum_1^N \frac{|U_{exp}-U_{pred}|}{U_{exp}}\times 100 \quad (11)$$

Table 1
Characteristics of inner surface roughness

Tube Inner Dimension	R_a (µm) Arithmetic Mean Roughness	R_v (µm) Max. Valley Depth	R_p (µm) Max. Peak Height
1.70 mm	0.21	-0.73	0.80

5. Results and Discussion

Figure 3 shows the typical boiling curve for 100 kg/m^{2}s at saturation temperature of 23 ^{o}C. The boiling curve is plotted for one mass flux to show clearly the dryout occurrence. A first change of slope in the boiling curve is the point where the incipience of dryout occurs as dryout patches are temporarily formed. These dryout patches are rewetted by the coming

waves of liquid and this wetting and rewetting continues until complete dryout occurs at the last thermocouple position. Above the dryout incipience heat flux, heat flux is increased in small steps and long enough time is allowed before recording data. These small steps are repeated until the wall superheat at the last thermocouple position overshoots above 25K. The power applied to the test section is cut off at this point to save the test section from burnout.

Table 2

Operational Conditions and Uncertainties

Parameter	Operating Range	Uncertainty
D (mm)	1.70	± 0.007
L_{hs} (mm)	245	± 0.2
G (kg/m^{2}s)	100- 500	± 3.5 %
q´´ (kW/m^2)	5-276	± 2.5 %
T_{sat} (^{o}C)	23,33,43	± 0.2
x	0-1.1	± 6 %

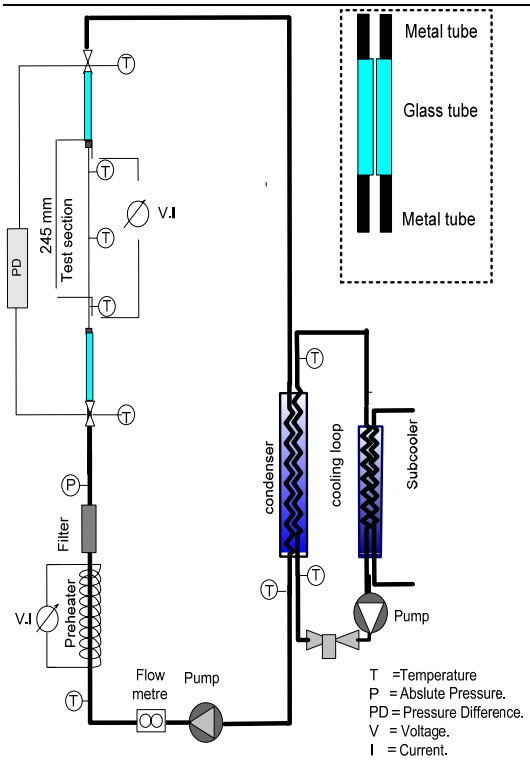

Fig 1: Schematic Diagram of test rig.

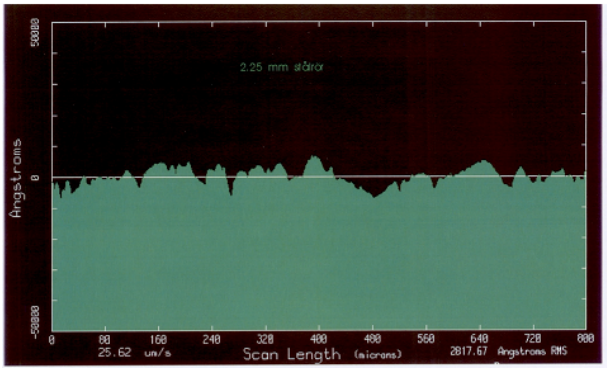

Fig. 2: Characterization of inner surface roughness of test section.

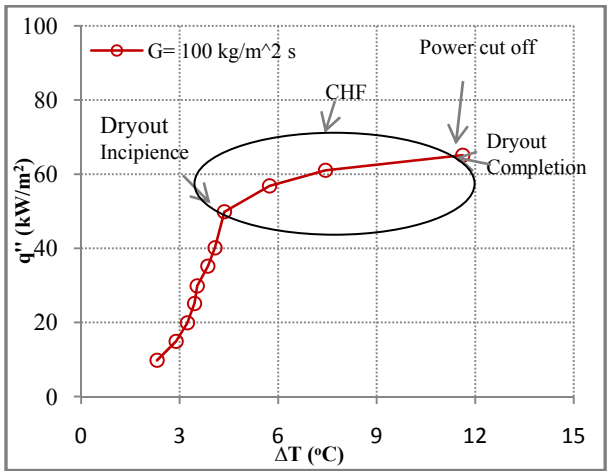

Fig.3: Boiling Curve and Identification of Dryout Incipience and Dryout Completion

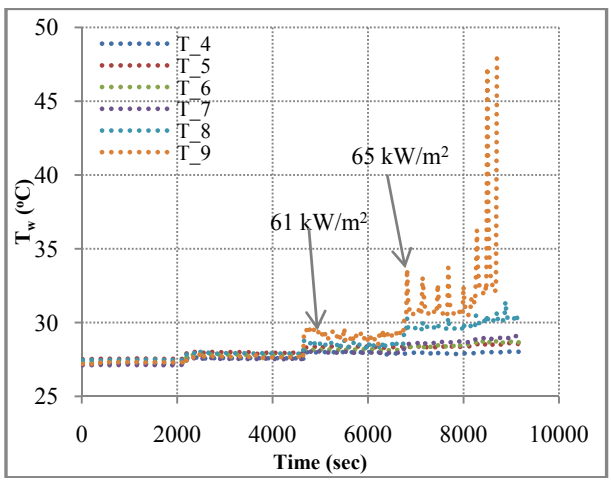

Fig.4: Temperature profiles near dryout for the last six thermocouples versus time.

The occurrence of dryout can also be shown by the temperature profiles of the thermocouples. Figure 4 shows the temperature profiles of the last six

thermocouples for mass flux of 100 kg/m^{2}s at a saturation temperature of 23 ^{o}C as a function of recording time. As can be seen from the figure, large fluctuations in the last two thermocouple readings indicate dryout behavior. The effect of these large fluctuations is an increase in the standard deviation in the temperature readings on the downstream side of the test section from the steady state standard deviation. Ali (2010) and Callizo et al. (2008) also reported similar trends at the occurrence of dryout.

Dryout heat flux as a function of mass flux at all saturation temperatures is presented in Figure 5. It can be seen that for a given saturation temperature, the dryout heat flux increases with increase in mass flux almost linearly. To reach dryout vapour qualities, higher heat flux is needed for higher mass flux. Different authors in previous studies of CHF in the literature such as Wojtan et al. (2006), Kosar and Peles (2007), Callizo et al. (2008) and Ali (2010) also reported similar trends.

It can also be seen from figure 5 that the saturation temperature has insignificant effect on dryout heat flux. The decrease in liquid to vapour density ratio with saturation temperature is expected to reduce the droplet entrainment rate in the vapour core which may increase dryout heat flux (Ali, et. al. 2010). At the same time the decrease in surface tension and latent heat of vaporization with increasing saturation temperature tends to reduce dryout heat flux (Kosar and Peles, 2007). These two contrary effects may be the reason that the effect of saturation temperature on dryout heat flux is diminished.

Dryout heat flux as a function of vapour quality is plotted in Figure 6 for mass fluxes ranging from 200 to 400 kg/m^{2}s at three saturation temperatures. For a particular data point, the point with the lower vapour quality corresponds to incipience of dryout and the point with the higher vapour quality corresponds to dryout completion. For a given saturation temperature, generally dryout incipience and dryout completion occurs at lower vapour quality for higher mass flux. According to Wahib (2007) and Ali (2010), the flow regime at dryout completion is annular. It has been suggested that, in annular flow, an increase in mass flow increases the droplet entrainment in the vapor core (Carey, 1992) thereby reducing the amount of liquid in the film (at a given vapor fraction), and thus also the film thickness. The liquid film may then break due to this droplet entrainment and the channel wall can be exposed to the vapor. This can be a reason for the decrease in dryout completion vapor quality at higher mass fluxes. Dryout vapor quality is observed to

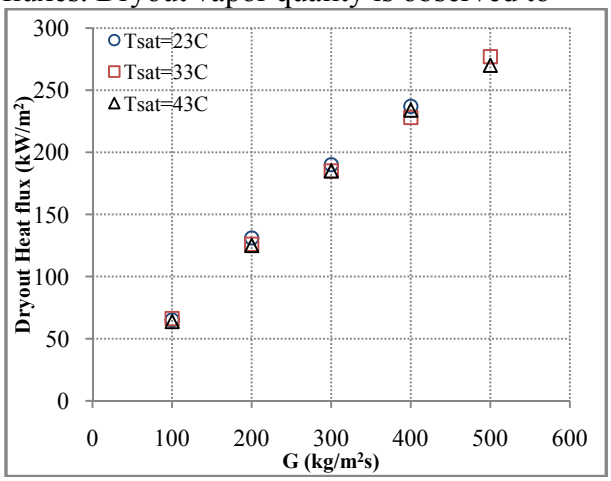

Fig. 5: Dryout Heat Flux versus mass velocity at three saturation temperatures.

increase with increase in saturation temperature which can be explained by the increase of vapor to liquid density ratio with saturation temperature which can reduce the droplet entrainment rate in the vapour core resulting in a delay of dryout (Ali, 2010). Again it can be seen from figure 6, that the effect of the saturation temperaure on dryout heat flux is insignificant.

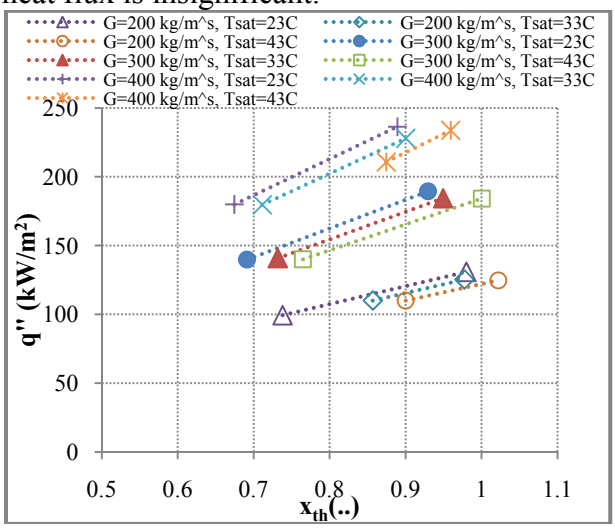

Fig. 6: Dryout Heat Flux versus vapour quality

6. Comparison with Correlations

The experimental dryout heat flux data is compared with well known macro and micro scale CHF correlations.

Figure 7 shows the comparison of the experimental data with Katto and Ohno correlation (1984). This correlation was originally developed for macro channels but as can be seen it predicts the data reasonably well with MAD of 15% where about 79% of the data is within ±20% range.

Bowring (1972) developed a CHF correlation for large diameter tubes. The experimental data is also compared with this correlation and is found to predict the data with a MAD of 13% and 100% of the experimental data points are in the ±20% range. The predictions of Bowring correlation (1972) are presented in Figure 8.

The correlation by Callizo et al. (2008) gave the best predictions among the correlations investigated in this article with MAD of 9 % and 100 % of the experimental data is within ±20 % range. Results are shown in Figure 9.

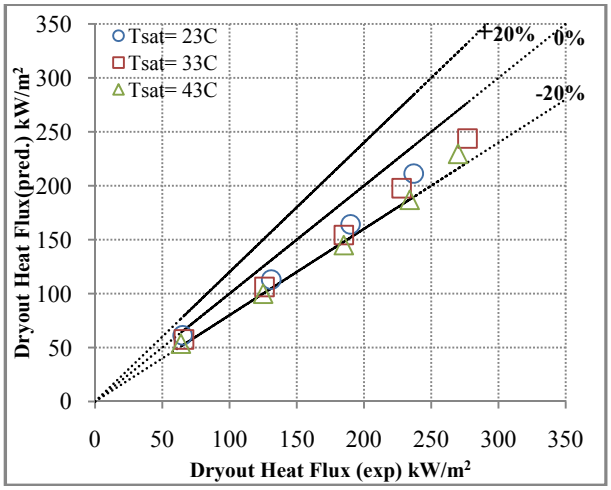

Fig. 7: Comparison of experimental data with Katto and Ohno correlation (1984).

The experimental data is also compared with Wojtan et al. (2006), Zhang et al. (2006), Qi et al. (2007) and Bowers and Mudawar (1994) correlations. A summary of the findings for all correlations is presented in table 3.

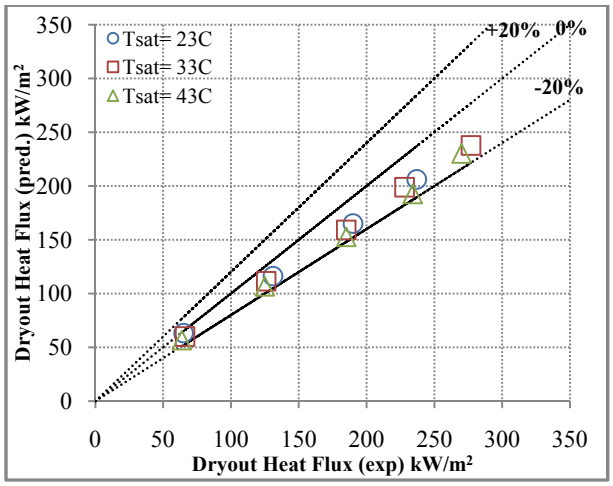

Fig. 8: Comparison of experimental data with Bowring correlation (1972).

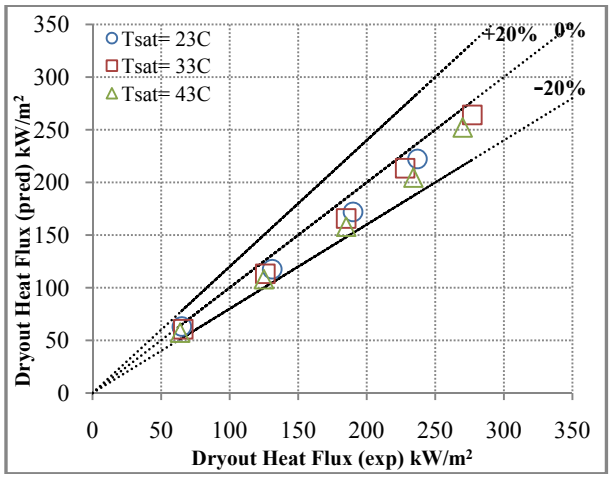

Fig. 9: Comparison of experimental data with Callizo et al. (2008).

Table 3

Assessment of Correlations

Correlation	MAD (%)	% of data within ±20%
Katto and Ohno (1984)	15	79
Bowring (1972)	13	100
Callizo (2008)	9	100
Wojtan et al. (2006)	35	22
Zhang et al. (2006)	21	43
Qi et al. (2007)	37	50
Bowers and Mudawar (1994)	19	72

Conclusions

Experiments have been performed to determine the dryout characteristics of propane in a vertical circular mini channel of 1.70 mm internal diameter at a heated length of 245 mm. The experiments were conducted at three saturation temperatures and for mass fluxes ranging from 100 kg/m^{2}s to 500 kg/m^{2}s.

The experimental results show that the dryout heat flux increases with increase of mass flux and with the decrease of vapour quality. It has also been observed that the saturation temperature has insignificant effect on the dryout heat flux at least for the experimental conditions considered in this study.

The experimental results are compared with existing correlations from the literature. Modified Kato and Ohno (1984) correlation Suggested by Callizo et al. (2008), Bowring (1972) and also Katto and Ohno (1984) correlation (1984) predicted the experimental results reasonably well.

Nomenclature

A	Area (m^2)
C_p	Specific heat (J/kgK)
D	Diameter (m)
G	Mass flux (kg/m^{2}s)
i_{lv}	Latent heat of vaporization (J/kg)
Δi_{in}	Inlet subcooling enthalpy (J/kg)
L	Length (m)
N	Number of points
q´´	Heat flux (kW/m^2)
T	Temperature (^{o}C)
U	Data point (--)
z	Axial length (m)

Greek letters

ρ	Density (kg/m^3)
σ	Surface tension (N/m)
μ	Viscosity (Ns/m^2)
x	Vapour quality (--)

Dimensionless numbers

Co	Confinement number $\left(\frac{\left(\frac{\sigma}{g(\rho_l-\rho_v)}\right)^{0.5}}{D}\right)$
We_D	Weber Number $\left(\frac{G^2 D}{\rho\sigma}\right)$
We_l	Weber Number $\left(\frac{G^2 L}{\rho\sigma}\right)$

Subscripts

c	Cross sectional
CHF	Critical heat flux
exp	Experimental
h	Hydraulic
hs	Heated section
in	Inlet
l	Liquid
pred	Predicted
sat	Sat
sub	Subcooled
v	Vapour

References

Ali R., 2010. Phase change phenomena during fluid flow in micro channels. *Doctoral Thesis in KTH Stockholm,* ISBN 978-91-7415-829-8.

Bowers M. B., Mudawar I., 1994. High flow boiling in low flow rate, low pressure drop mini-channel and micro-Channel heat sinks, *Int. J. of Heat and Mass Transfer* 37, 321-332.

Bowring R. W., 1972. A simple but accurate round tube uniform heat flux correlation over the pressure range 0.7-17 MN/m^2, *Report AEEW-R789, Winfrith,UK.*

Callizo C. M., Ali R., Palm B., 2008. Dryout incipience and critical heat flux in saturated flow boiling of refrigerants in a vertical uniformly heated microchannels, *Proc. of the 6th Int. ASME Conf. on Nanochannels, Microchannels and Minichannels, ICNMM2008, Darmstadt Germany.*

Carey, V.P., 1992. Liquid-vapor phase change phenomena, *Hemisphere, New York*, 483-564.

Collier J. G., Thome. J. R., 1994. Convective boiling and condensation, 3rd edition *Oxford university press*, pp.171.

Fernando P., Palm B., Ameel T., Lundqvist P., Granryd E., 2007. A minichannel aluminium tube heat exchanger –Part 2: evaporator performance with propane. *Int. J. of refrigeration*, 31(4), 681-695.

Katto Y., Ohno H., 1984. An improved version of the generalized correlation of critical heat flux for forced convective boiling in uniformly heated vertical tubes, *Int. J. of Heat and Mass Transfer*, 27, 1641-1648.

Kosar A., Peles Y., 2007. Critical heat flux of R123 in silicon based microchannels, *ASME J. of Heat Transfer,* 129 (7), 844-851.

Lazarek G. M., Black S. H. 1982. Evaporative heat

transfer, pressure drop and critical heat flux in a small vertical tube R-113, *Int. J. of Heat and Mass Transfer,* 25, 945-960.

Owhaib W., 2007. Experimental heat transfer, pressure drop and flow visualization of R-134a in vertical mini/micro tubes, *Doctoral Thesis in KTH Stockholm,* ISBN 978-91-7178-594-7.

Qi S.L., Zhang P., Wang R. Z., Xu L. X., 2007. Flow boiling of liquid nitrogen in micro tubes: Part II- heat transfer characteristics and critical heat flux, *Int. J. of Heat and Mass Transfer* 50, 5017-5030.

Tain R. M., Cheng S. C., Groeneveld D. C., 1993. Critical heat flux measurements in a round tube for CFCs and CFC alternatives. *Int. J. of Heat and Mass Transfer* 36 (8), 2039-2049.

Taylor B.N., Kuyatt C.E., 1994. Guidelines for evaluating and expressing the uncertainty of NIST measurement results, National Institute of Standards and Technology Technical Note 1297.

Wojtan L., Revellin R., Thome J. R., 2006. Investigation of saturated critical heat flux in a single,uniformly heated microchannel. *Exp. Thermal and Fluid Sci.,* 30, 765-774.

Zhang W., Hibiki T., Mishima K., Mi Y., 2006. Correlation of critical heat flux for flow boiling of water in mini-channels, *Int. J. of Heat and Mass Transfer* 49, 1058-1072.